Korean J. Chem. Eng., 32(9), 1835-1841 (2015)
DOI: 10.1007/s11814-014-0390-y

pISSN: 0256-1115
eISSN: 1975-7220

Synthesis of ordered mesoporous SBA-15 and its adsorption of methylene blue

Anaam Akram Sabri, Talib Mohammed Albayati†, and Raghad Adnan Alazawi

Department of Chemical Engineering, University of Technology, 52 Alsinaa St., P. O. Box 35010, Baghdad, Iraq
(*Received 8 October 2014 • accepted 26 December 2014*)

Abstract−The removal of methylene blue (MB) dye pollutant from synthetic wastewater onto mesoporous SBA-15 was studied in batch adsorption systems. The characterization for the prepared adsorbent such as: X-ray diffraction (XRD), scanning electron microscopy (SEM), BET surface area and Fourier transform infrared (FTIR) spectroscopy was achieved. The experiments were carried out to measure the adsorption capacity as a function of contact time, initial concentration (40-110 mg/L), pH (3-11) and adsorbent dose (0.1-2.3 g/L). The equilibrium of the process was achieved within 20 min. Adsorption isotherms were fitted with the Langmuir, Freundlich and Temkin models. The equilibrium data were better represented with Langmuir Isotherm model. The kinetics of the MB sorption on SBA-15 was examined by using pseudo-first and pseudo-second order kinetics models. The kinetics analysis showed that the overall adsorption process was successfully fitted with the pseudo-second-order kinetic model. Good linearization of the data was observed for the initial phase of the reaction in accordance with expected behavior of intraparticle diffusion as the rate-limiting and rate-controlled step. SBA-15 can be effectively recovered by calcinations and reused fourteen times in batch system without significant loss in removal of methylene blue from aqueous solution.

Keywords: Waste Water Treatment, Mesoporous SBA-15, Methylene Blue, Batch Adsorption, Organic Pollutants

INTRODUCTION

Organic dyes are an integral part of many industrial effluents. Over 7×10^5 tons and approximately 100,000 different dyes are produced annually worldwide [1]. The level of the dye pollutants even in very low concentration is highly visible and will affect aquatic life as well as the food web. Methylene blue (MB) (methylthionine chloride) is one of the basic dyes. It is employed in some medical uses in large quantities; it can also be widely used in coloring paper, dyeing cottons, wools, coating paper of stocks, etc. Although MB is not strongly hazardous, it can cause some harmful effects. Acute exposure to MB causes increased heart rate, vomiting, shock, Heinz body formation, cyanosis, jaundice and quadriplegia and tissue necrosis in humans [2,3]. Many dyes have high stability to light, temperature and are not biologically degradable [4]. Due to low biodegradability of dyes, a conventional biological treatment process is not very effective in treating a dye wastewater [5]. It is usually treated by physical and/or chemical methods such as coagulation, filtration, precipitation, ozonation, adsorption, ion exchange, reverse osmosis and advanced oxidation processes [6,7]. Among the various techniques, adsorption is very popular due to simplicity of design and operation, insensitivity of toxic substances, and the possibility to operate at very low concentration [8,9]. Several adsorbents have been tested for dye removal, such as activated carbon, alumina, fly ash, clays, silica gel, and zeolite. Zeolites were treated special attention in sorption process [10]. However, their inherent small pore size creates a key limitation to their applications as larger molecules are not able to access their pores. Hence, mesoporous silica was developed in the wake of this limitation [11]. The greatest advantage of these materials is their large surface area, uniform pore size, controlled surface chemistry, and their adsorption - regeneration properties. SBA-15 is a highly ordered material possessing a regular two-dimensional hexagonal array of channels. This material typically has a pore diameter of the order of (4-14 nm) [12].

In this study, SBA-15 mesoporous silica was synthesized and characterized to use as adsorbent to remove the methylene blue (MB) dye from synthetic wastewater in batch adsorption system. The study included the effect of adsorbent dose, contact time, initial MB concentration and PH on the uptake of methylene blue; also a study of the adsorption isotherm of the experimental data and the kinetic models to predict the adsorption rate constants. Regeneration of SBA-15 will achieve to explore the practical usefulness of the adsorbent and its possible reuse in batch sorption process.

MATERIALS AND METHODS

1. Chemicals

The reactants used in this study were poly (ethylene glycol)-block-poly (propylene glycol)-block-poly (ethylene glycol) [Pluronic P123, $(C_3H_6O{\cdot}C_2H_4O)_x$, MW=5,800 g/mol] as a surfactant and tetraethyl orthosilicate (TEOS, $(C_2H_5O)_4$ Si, MW=208.33 g/mol) as a silica source; these chemicals were purchased from Sigma Aldrich Company. Hydrochloric acid (HCl, 37%), sulfuric acid (H_2SO_4, 95%-98%) were provided by Biosolve-USA, sodium hydroxide (NaOH, 99%) was purchased from BDH England and methylene Blue (MB, MW=319.8 g/mol) was provided by HiMedia India.

2. Synthesis of SBA-15 Mesoporous Silica

SBA-15 was synthesized as reported by [13-15]. 6.0 g of Pluronic P123 was dissolved in 45 g of water and 180 g of 2 M HCl solution. Subsequently, 12.75 g of silica precursor (TEOS) was added to

†To whom correspondence should be addressed.
E-mail: talib_albyati@yahoo.com

the solution. The resulting mixture was stirred for (24 h) at 35 °C and then aged by oven at 100 °C for 24 h. Then, the mixture was allowed to cool at room temperature and the white solid product was filtered, washed with distilled water for removing partial surfactant and dried at room temperature for 3 h. Calcination was performed at 550 °C for 6 h in a furnace to remove the surfactant template. Finally, a white powder (SBA-15) was obtained.

3. Preparation of Adsorbate Solution

The stock solution was prepared by dissolving 1g of methylene blue in distilled water and made up to the 1,000 ml stock solution in volumetric flask. From the stock, different concentrations (15-110 mg/*l*) of methylene blue were prepared by diluting with distilled water.

4. Characterization of Adsorbents

The small angle XRD patterns were recorded under ambient conditions with a Philips 1830 powder X-ray diffractometer (XRD-6000 Shimadzu, Japan), using the Cu-Kα radiation source of wavelength (λ=1.5406 Å) a ranging from - 4.0000 to 20.0000 deg. The X-ray tube was operated at 40 kV and 30 mA while the data were recorded in the 2θ range of 0.5-6° with a 2θ step size is 0.0200 deg and a step time of 0.10 sec. The surface morphology of the mesoporous materials was obtained by scanning electron microscopy (SEM, TESCAN Germany). The specific surface areas of the samples were calculated using the Brunauer-Emmett-Teller (BET) method (BET, Q-surf 9600 USA). Fourier transform-infrared spectra (FT-IR) spectroscopy is a technique that provides information about the chemical bonds between molecules and the functional groups grafted onto the SBA-15 solid samples, diluted in (8 wt%) KBr which were recorded at room temperature in transmission mode in the range of 4,000 to 400 cm^{-1} at 4 cm^{-1} resolution regions by using (FT-IR, Bruker-Tensor 27, Germany) spectrometer.

5. Batch Adsorption Experiments

Batch adsorption experiments were performed in 100 ml conical flasks containing 100 ml of MB solution of known concentration and pH. A known quantity of adsorbent was added in the 100 ml flasks at room temperature. The mixture was stirred by electrical shaker at 200 rpm. An equilibrium study was carried out by taking the sample from the shaker at regular intervals of 10 min. In each sample, the adsorbent was separated by centrifuge at 2,080 rpm for 20 min and filtering by filter paper. The absorbance of the supernatant solution was estimated to determine the residue of dye concentration. The removal efficiency was calculated by the following equation [16]:

$$R\% = \frac{C_0 - C_t}{C_0} \times 100\% \quad (1)$$

where R is the removal efficiency and C_0 is the initial concentration and C_t the concentration in mg/*l* at t time.

6. Effect of Contact Time

To find the effect of contact time (0.01) g of SBA-15 sample was mixed with 100 ml of the aqueous solutions with initial concentrations 40 mg/*l* of MB. The flasks with their contents were shaken for the different adsorption times (1-60) min at pH 7.

7. Effect of Adsorbent Dosage

In the batch sorption experiments the effect of the dose of SBA-15 (0.1-2.3) g/*l* adsorbent on adsorption of MB of 40 mg/*l* concentration and pH 7 was studied with contact time of 20 min.

8. Effect of Initial Dye Concentration

The initial concentration of MB solution was varied from (15-110) mg/*l* and batch experiments were carried out with 0.2 g of SBA-15 at solution pH 7 for 20 min.

9. Effect of pH

The effect of initial pH on adsorption of MB was examined over a range of pH values from (3-11) adjusted by 0.1 M H_2SO_4 or 0.1 M NaOH through taking 100 ml of 15 mg/*l* MB dye solutions with 0.2 g of SBA-15 for 20 min shaking.

10. Adsorption Isotherm

The equilibrium adsorption isotherm is fundamental in describing the interactive behavior between adsorbate and adsorbent, and it is important in the design of adsorption systems. The adsorption isotherm was studied at different dose of SBA-15 (0.1-2.3) g/*l* with 40 mg/*l* MB solutions and pH 7. The adsorption data for MB was fitted into Langmuir, Freundlich and Temkin isotherms equations. The linearization form of the Langmuir equation [17] is as follows:

$$\frac{C_{eq}}{q_e} = \frac{1}{q_m} C_{eq} + \frac{1}{K_L q_m} \quad (2)$$

where q_m is the Langmuir constant relating to adsorption capacity mg/g. K_L is the constant that refers to energy of adsorption *l*/mg. The constants q_m and K_L can be determined from a linearization form of Eq. (3) by the slope of the linear plot of C_{eq}/q_e versus C_{eq}.

The linear form of the Freundlich equation is given by [18]:

$$\ln q_e = \ln K_f + \frac{1}{n} \ln C_{eq} \quad (3)$$

where K_f and l/n are Freundlich constants related to adsorption capacity and adsorption intensity, respectively of the sorbent. The values of K_f and l/n can be obtained from the intercept and slope, respectively, of the linear plot of experimental data of $\ln q_e$ versus $\ln C_{eq}$.

Temkin isotherm is represented by the following equation [19]:

$$q_e = B \ln K_t + B \ln C_{eq} \quad (4)$$

where constant $B = R_e T/b$. The adsorption data were analyzed according to Eq. (4). A plot of q_e versus $\ln C_{eq}$, enables the determination of the isotherm constants K_t and B.

11. Adsorption Kinetics

The kinetics study was carried out using 0.01 g of SBA-15 in 100 ml of 40 mg/*l* MB solution at pH 7. The rate of sorption is analyzed by three kinetic models, namely pseudo-first-order, pseudo-second-order and Intraparticle diffusion, which are expressed by Eqs. (5), (6) and (7), respectively.

$$\log(q_t - q_e) = \log q_e - \frac{k_{1ads}}{2.303} t \quad (5)$$

where k_{1ads} is the rate constant of the pseudo-first-order model in (min^{-1}) and q_t is the amount of adsorption at time t in (mg/g). The adsorption rate constant, k_{1ads} can be experimentally determined by the slope of linear plots $\log(q_t - q_e)$ vs. t [20]:

$$\frac{t}{q_t} = \frac{1}{k_{2ads} q_e 2} + \left(\frac{1}{q_e}\right) t \quad (6)$$

where k_{2ads} is the rate constant of the pseudo-second-order in (g/

mg min). The value of $k_{2ads}q_e2$ can be obtained from the intercept and slope of plotting t/q_t vs. t [21]:

$$q_t=k_i t^{0.5}+C_i \quad (7)$$

where k_i is a measure of diffusion coefficient in (mg/g $min^{0.5}$) and C_i is intraparticle diffusion constant, i.e., intercept of the line (mg/g). It is directly proportional to the boundary layer thickness. The k_i values under different conditions were calculated from the slopes of the straight line portions of the respective plots [22].

12. Regeneration of SBA-15

The regeneration experiments were carried out by calcination of SBA-15 at 550 °C after each cycle. In these experiments 0.2 g of SBA-15 was first treated with 100 ml of MB solution with concentration 40 mg/*l* in pH=7, at the end of adsorption the adsorbent was regenerated and then reused in the next run under the same conditions for fourteenth runs.

RESULTS AND DISCUSSIONS

1. Characterization of Adsorbents

The small angles of X-ray diffraction (XRD) patterns of SBA-15 sample are shown in Fig. 1. This figure displays intense diffraction three peaks, a single strong peak (1 0 0) at about 2θ of 0.9 which is characteristic of a mesostructure. Moreover, followed by two small peaks which can be indexed as (1 1 0) and (2 0 0). The characteristic peaks suggest as structure of p6mm symmetry, which is a typical of uniform mesopore structure with hexagonal order. The peaks obtained in this study match very well with the similar peaks reported in the literatures [23,24].

The results demonstrate that the ordered structure of SBA-15 was maintained after the regeneration process.

The morphology of the SBA-15 was analyzed by a scanning electron microscope as shown in Fig. 2. This figure shows that SBA-15 has the typical wheat-like morphology and consists of aggregates of rope-like particles with relatively uniform size [25,26].

The BET surface area, pore volume, pore diameter and real density of SBA-15 were measured and summarized in Table 1. These results showed that the prepared mesoporous material SBA-15 with higher surface area and pore volume falls within the range of surface area (400-900 m^2g^{-1}) and pore volume (0.56-1.23 cm^3/g) for SBA-15 [27]. The structural parameters calculated from nitrogen adsorption measurements are presented in Table 1. The specific surface area, pore volume and pore size of the samples followed the order: SBA-15>regenerated sample of SBA-15, whereas a different order was observed in terms of wall thickness. The significant decreases in the surface area of the loaded samples in comparison with regenerated SBA-15 confirm the attachment of MB residue particles inside the pores.

The FT-IR spectrum for SBA-15 is shown in Fig. 3. The peaks at 1,063 and 460 cm^{-1} are assigned to silanol groups Si-O-Si bands. Also, the peaks at around 930, 810, 3,400 cm^{-1} and small peak at 2889 could be assigned as the Si-OH banding and at a peak around 1,600 cm^{-1} assigned to O-H [28-30]. A regenerated sample of SBA-15 exhibits a very similar spectrum to SBA-15, generally due to its low MB content, except for exhibiting one additional band at 2,400 cm^{-1}. We attribute this to the presence of residue particles of MB on the external surface of the pores.

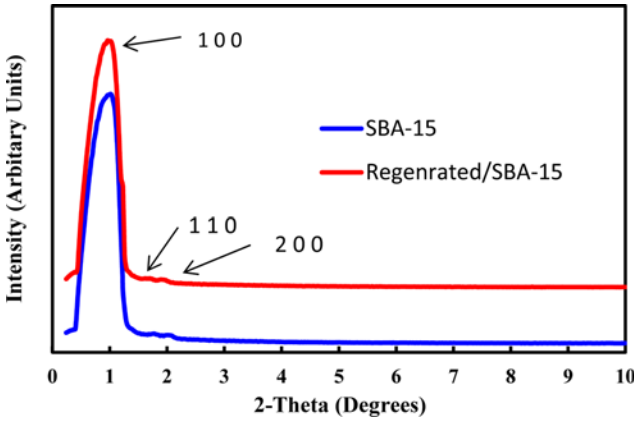

Fig. 1. XRD diffraction patterns for SBA-15 and regenerated SBA-15.

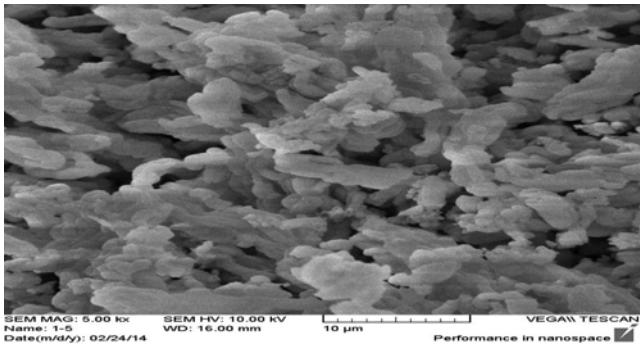

Fig. 2. SEM image of SBA-15 at a magnification of 10,000.

Table 1. The structure properties of nanoporous material SBA-15

Material	S_{BET} (m^2/g)	V_P (cm^3/g)	Vμp (cm^3/g)	DP (nm)	α_0 (nm)	t_{wall} (nm)	ρ (g/cm^3)
SBA-15	790.83	0.976	0.789	8.1	10.93	2.95	3.62
Regenerated SBA-15	750.27	0.897	0.813	7.8	10.73	3.15	3.45

Notes: SBET is the surface area determined using the BET method between the relative pressures (P/P0) 0.05-0.25. VP and VμP are the total pore volume and micropore volume, respectively, obtained using the t-plot method. The total pore volume was estimated from the amount adsorbed at a relative pressure of 0.97. DP is the pore diameter calculated by means of the BJH method from the adsorption branch of the isotherm. α0 is the unit cell parameter calculated by XRD, being α0 ¼ 2d100/√3. twall is the wall thickness calculated using the equation twall ¼ α0 - DP. P is the real density [24]

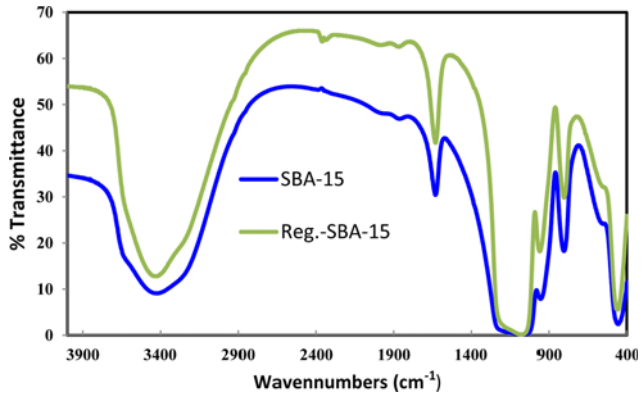

Fig. 3. FT-IR spectra for SBA-15 and regenerated SBA-15.

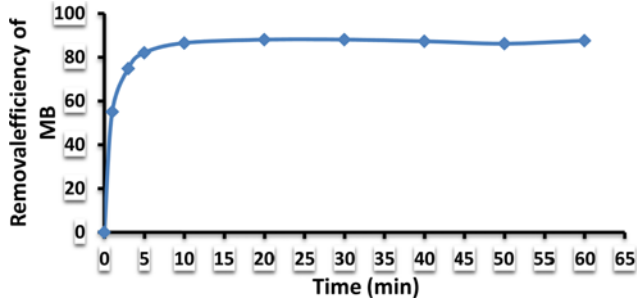

Fig. 4. Effect of contact time on the removal efficiency of MB (C_o= 40 mg/*l*, pH=7, SBA-15 dosage=0.01 g).

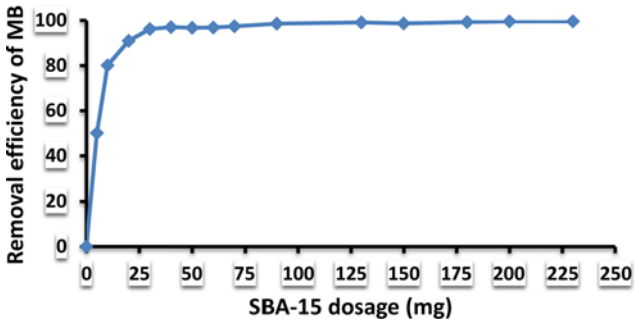

Fig. 5. Effect of adsorbent dose on the removal efficiency of MB (C_o= 40 mg/*l*, pH=7, contact time=20 min).

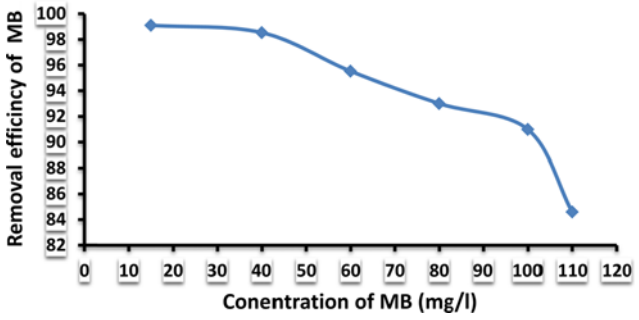

Fig. 6. Effect of initial MB concentration on removal efficiency (pH= 7, contact time=20 min, SBA-15 dosage=0.2 g).

2. Adsorption of Methylene Blue in Batch System

2-1. Effect of Contact Time

The effect of contact time on the removal efficiency of MB was studied at initial concentration of MB (C_o=40 mg/*l*, pH=7, SBA-15 dosage=0.01 g) as shown in Fig. 4. The removal efficiency of MB is rapid in the first minutes of contact time and after 20 min the removal does not vary significantly.

This can be explained that a large number of vacant surface sites are available for the adsorption at the beginning. It was also suggested that a strong attractive force occurred between the dye molecules and the sorbent, and with an increase in contact time, the remaining vacant surface sites are difficult to be occupied due to saturation occurring. This may be due to the deficient number of available sorption sites at the end of the sorption process, so the removal efficiency remained almost constant [31].

2-2. Effect of Adsorbent Dose

The experiment was performed to establish appropriate adsorbent dose for MB removed by increasing the amount of SBA-15 added to 100 ml of 40 mg/*l* MB solution. It can be seen from Fig. 5 that the removal efficiency of MB removed at (25) mg of SBA-15 was (95%) and the removal efficiency was increased with increasing sorbent amount until reaching (99.5%) removal efficiency of MB at (200) mg of SBA-15. The increase in removal efficiency with the adsorbent dosage can be attributed to the availability of greater surface area with pore volume and larger number of adsorption sites [32].

2-3. Effect of Initial MB Concentration

The effect of initial MB concentration is shown in Fig. 6. The removal efficiency decreased with the increase in the MB concentration from 10 to 110 mg/*l*, due to the increase of the ratio of the dye's cations to the dosage of the adsorbent and the number of active adsorption sites required to accommodate the remaining adsorbate while the number of adsorbate increases and hence the removal efficiency of the adsorption decreases [33,34].

2-4. Effect of pH

MB removal was studied at different pH ranging between 3 and 11. The PH was adjusted with (0.1 N) of H_2SO_4 and NaOH solution. The maximum removal efficiency was at pH 7 as shown in Fig. 7. The removal efficiency decreased in acidic pH but remained almost constant in basic conditions. The observed low adsorption of MB onto SBA-15 at pH<7 is probably due to the presence of excess (H^+)

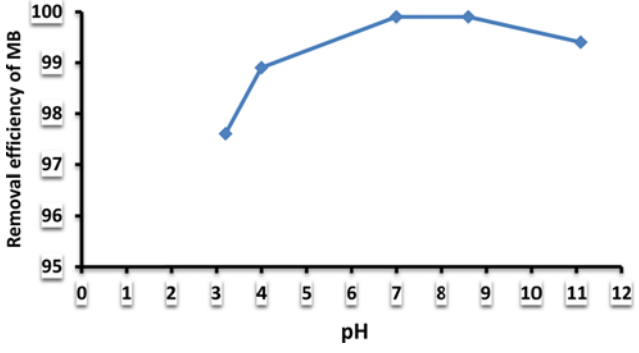

Fig. 7. Effect of pH on the removal efficiency of MB (C_o=15 mg/L, contact time=20 min, SBA-15 dosage=0.01 g).

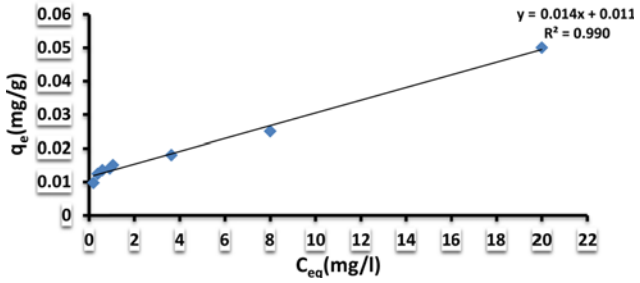

Fig. 8. Langmuir isotherm model.

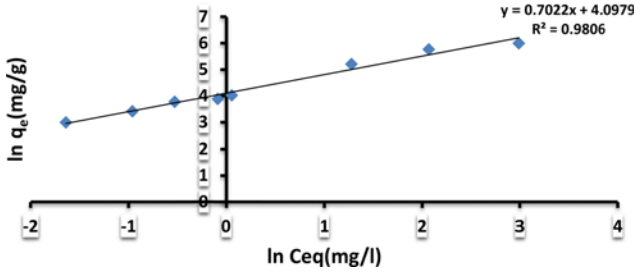

Fig. 9. Freundlich isotherm model.

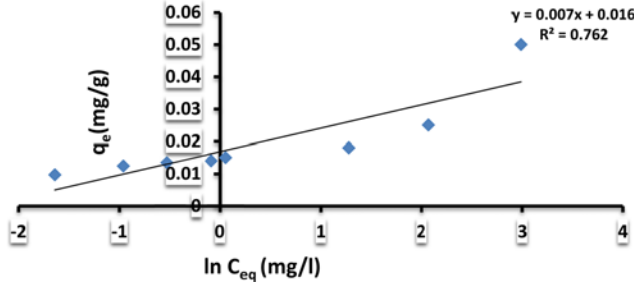

Fig. 10. Temkin isotherm model.

ions competing with MB cationic group for adsorption sites, causing a decrease in the amount of MB adsorbed. However, the concentration of MB quickly decreased as removal by adsorbent SBA-15 proceeded at pH≥8; the surface of SBA-15 becomes negatively charged, so the binding of positively charged dyes onto these surfaces becomes very favorable, resulting in enhanced adsorption of dye [35].

2-5. Adsorption Isotherms

The linearized Langmuir, Freundlich, and Temkin plots are given in Figs. 8, 9 and 10, respectively. The isotherm constants and R^2 for each model are given in Table 2. Table shows the correlation coefficients values (0.990, 0.980, and 0.762) for Langmuir, Freundlich and Temkin models, respectively. These values were indicated that the Langmuir isotherm having higher correlation coefficient compared with Freundlich and Temkin models and that shows a better fitting model with experimental data [36].

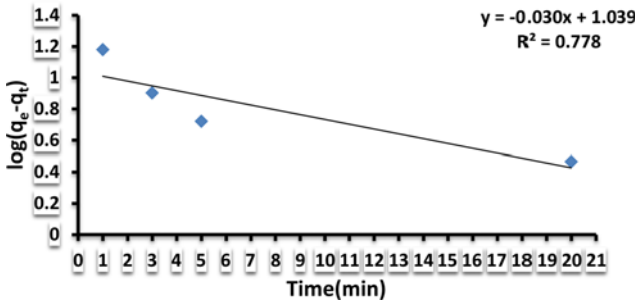

Fig. 11. Pseudo-first order kinetics models.

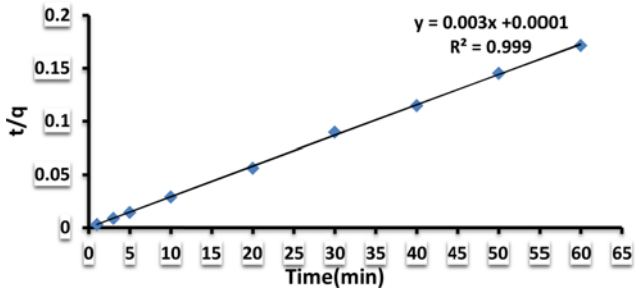

Fig. 12. Pseudo- second order kinetics models.

2-6. Adsorption Kinetics

The rate of MB adsorption by SBA-15 was one of the significant factors that define the efficiency of adsorption. The kinetics of the MB sorption on SBA-15 was examined by using pseudo-first and pseudo-second-order kinetics models as shown in Figs. 11 and 12. The parameters values of the kinetic models and the correlation coefficients (R^2) are listed in Table 3. The theoretical ($q_{e\,cal.}$) values estimated from the pseudo-first-order kinetic model gave significantly different value compared to experimental ($q_{e\,exp.}$) value as shown in Table 3; therefore, the pseudo-first-order kinetic model did not describe well this adsorption system. While Table 3 shows

Table 2. Isotherm parameters for MB adsorbed onto SBA-15 with the correlation coefficient

Isotherms	Langmuir			Freundlich			Temkin		
	q_m (mg/g)	K_L (L/mg)	R^2	K_F ($mg^{1-n}g^{-1}L^n$)	1/n	R^2	K_t (L/mg)	B	R^2
SBA-15	71.42	1.27	0.990	60.15	0.702	0.980	9.77	0.007	0.762

Table 3. Kinetic adsorption parameters obtained by using pseudo-first-order and pseudo-second-order models

Adsorbent	$q_{e.exp}$ (mg g^{-1})	Pseudo-first-order			Pseudo-second-order		
		$q_{e.cal}$ (mg g^{-1})	k_{1ads} (min^{-1})	R^2	$q_{e.cal}$ (mg g^{-1})	k_{2ads} (g min^{-1} mg^{-1})	R^2
SBA-15	351	10.93	6.9×10^{-3}	0.778	333.3	9×10^{-2}	0.999

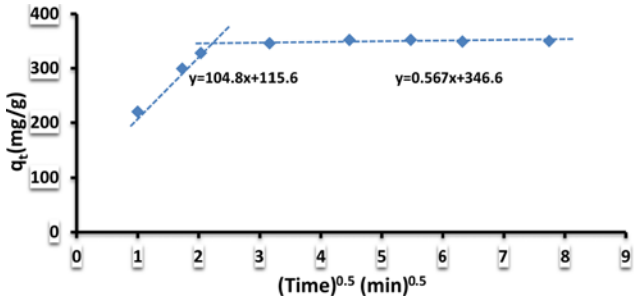

Fig. 13. Intraparticle diffusion of MB by SBA-15.

the theoretical ($q_{e\,cal.}$) values, estimated from the pseudo-second order kinetic model, are very close to the experimental ($q_{e\,exp.}$) value. Furthermore, the coefficients R^2 value is close to 1, confirming the applicability of the pseudo-second-order equation [37,38].

2-7. Intraparticle Diffusion

Fig. 13 shows the amount of dye adsorbed versus $t^{1/2}$ for intraparticle transport of MB by SBA-15. The line does not pass through the origin, indicating that the intraparticle diffusion is involved in the adsorption process, but it is not the only rate limiting mechanism and that the some other mechanisms also play an important role. The plot presents a multi linearity, which indicates that two steps occurred in the process. The first sharp section is the external surface adsorption or instantaneous adsorption stage with an intercept of 115.6 mg/g and k_{i1} was 104.8 mg/g·min$^{0.5}$. The second subdued portion is the gradual adsorption stage, where intraparticle diffusion is rate-controlled; the values of k_{i2} and intercept were 0.567 mg/g·min$^{0.5}$ and 346.6 mg/g, respectively. Thus, a combination of mechanisms was involved in the adsorption of MB dyes on SBA-15 adsorbent [39,40].

2-8. Batch Regeneration System

The regeneration process is considered as one of the most important features of the adsorption process, which reduces the process cost; therefore, the reuse experiments were carried out by calcination of the SBA-15 at 550 °C after each run and then reused in the next run under the same conditions so as to know how many times that can be reused SBA-15 as adsorbent to remove MB by regenerating it. The results of regeneration and recirculation of SBA-15 are shown in Fig. 14. This figure indicates that the removal efficiency of MB changed only from 99% to 94% after fourteen runs of regeneration of SBA-15. This means that SBA-15 can be easily regenerated and reused efficiently.

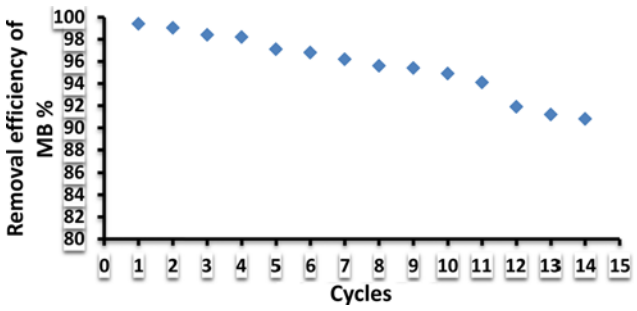

Fig. 14. The reusability of SBA-15 in batch experiment.

CONCLUSIONS

Nanoporous SBA-15 was prepared, characterized and used as adsorbent for the removal of MB from synthetic wastewater. It was found to have greater potential for the adsorption of methylene blue from aqueous solution in batch adsorption system. Batch experiment showed that the percentage of removal of MB increases with increase in the contact time, SBA-15 dosage, and pH, and decreases with increase in initial MB concentration. The adsorption isotherms studies demonstrated that the adsorption processes can be well fitted by the Langmuir isotherm model with a higher correlation coefficient (0.990). The adsorption kinetics of MB on to SBA-15 is well described by a pseudo-second-order kinetic model. In batch experiment SBA-15 can be easily regenerated and reused for 14 times with an effective application for the treatment of MB solution.

ACKNOWLEDGEMENTS

We would like to express our thanks to the Department of Chemical Engineering, University of Technology/Baghdad, Iraq for their financial support.

REFERENCES

1. M. Kharub, *J. Environ. Res. Development*, **6**(3A) (2012).
2. V. Vadivelan and K. V. Kumar, *J. Colloid Interface Sci.*, **286**, 90 (2005).
3. K. V. Kumar, V. Ramamurthi and S. Sivanesan, *J. Colloid Interface Sci.*, **284**, 14 (2005).
4. H. Benaissa, Thirteenth International Water Technology Conference, IWTC 13, 2009, Hurghada, Egypt, 377 (2009).
5. Y. Tian, X. Wang and Yufang, *J. Hazard. Mater.*, **213-214**, 361 (2012).
6. T. Hsu, *Fuel*, **87**, 3040 (2008).
7. Qusay F. Alsalhy, Talib M. Albyati and Mumtaz A. Zablouk, *Chem. Eng. Commun.*, **200**(1), 1 (2013).
8. F. K. Bangash and Abdul Manaf, *J. Chinese Chem. Soc.*, **52**, 489 (2005).
9. Talib M. Albayati, *Part. Sci. Technol.*, **32**, 616 (2014).
10. Talib M. Albayati and Aidan M. Doyle, *Chemistry: Bulgarian J. of Science Education*, **23**(1), 105 (2014).
11. Z. A. ALOthman, *Materials*, **5**, 2874 (2012).
12. N. Rahmat, A. Z. Abdullah and A. Mohamed, *American J. Appl. Sci.*, **7**(12), 1579 (2010).
13. D. Zhao, J. Feng, Q. Huo, N. Melosh, G. H. Fredrickson, B. F. Chmelka and G. D. Stucky, *Science*, **279**, 548 (1998).
14. Talib M. Albayati and Aidan M. Doyle, *Eng. Technol. J.*, **31**(18), 36 (2013).
15. Talib M. Albayati, Aidan M. Doyle, *Eng. Technol. J.*, **32**(4), 778 (2014).
16. Talib M. Albayati and Aidan M. Doyle, *Adsorpt. Sci. Technol.*, **31**(5), 459 (2013).
17. I. Langmuir, *J. Amer. Chem. Soc.*, **38**(11), 2221 (1916).
18. H. Freundlich, *Colloid and Capillary Chemistry*, **3**(12), 1454 (1926).
19. M. J. Temkin and V. Pyzhev, *Recent modifications to Langmuir isotherms*, Acta Physiochim, URSS, **12**, 217 (1940).

20. S, Afsaneh, Y. Habibollah and B. Alireza, *Chem. Eng. J.*, **168**, 505 (2011).
21. Y. S. Ho and G. McKay, *Process Biochem.*, **34**, 451 (1999).
22. W. J. Weber and J. C. Morris, *J. Sanit Eng. Div. ASCE*, **89**, 31 (1963).
23. S. Kuai and Z. Nan, *Chem. Eng. J.*, **244**, 273 (2014).
24. T. M. Albayati and A. M. Doyle, *Int. J. Chem. React. Eng.*, **12**(1), 1 (2014).
25. A. Shahbazi, H. Younesia and A. Badiei, *Chem. Eng. J.*, **168**, 505 (2011).
26. A. Arumugam and V. Ponnusami, *Indian J. Chem. Technol.*, **20**, 101 (2013).
27. T. Klimova, A. Esquivel, J. Reyes, M. Rubio, X. Bokhimi and J. Aracil, *Micropor. Mesopor. Mater.*, **93**, 331 (2006).
28. Q. Meng, X. Zhang, C. He, P. Zhou, W. Su and Ch. Duan, *Talanta*, **84**, 53 (2011).
29. T. X. Bui, S. Y. Kang, S. H. Lee and H. Choi, *J. Hazard. Mater.*, **193**, 156 (2011).
30. T. M. N. Albayati, S. E. Wilkinson, A. A. Garforth and A. M. Doyle, *Heterogeneous Alkane Reactions over Nanoporous Catalysts Transport in Porous Media*, **104**, 315 (2014).
31. R. Tang, Q. Lia, H. Cui, Y. Zhang and J. Zhai, *Polym. Adv. Technologies*, **22**, 2231 (2010).
32. L. Hajiaghababaei, A. Badiei, M. R. Ganjali, S. Heydari, Y. Khaniani and G. M. Ziarani, *Desalination*, **266**, 182 (2011).
33. M. B. Keivani, K. Zare, H. Aghaie and R. Ansari, *J. Phys. Theoret. Chem.*, **6**(1), 50 (2009).
34. Y. Dong, B. Lu, S. Zang, J. Zhao, X. Wang and Q. Cai, *J. Chem. Technol. Biotechnol.*, **86**, 616 (2011).
35. M. Anbia and S. A. Hariri, *Desalination*, **261**, 61 (2010).
36. M. Zendehdel, Z. Kalateh and H. Alikhani, *Iran. J. Environ. Health Sci. Eng.*, **8**(3), 265 (2011).
37. T. Santhi and S. Manonmani, *Sustain. Environ. Res.*, **22**(1), 45 (2012).
38. G. Mourchid, I. Maghri, M. Elkouali, A. Kenz, M. Talbi and A. Amougay, *Global J. Science Frontier Research Chemistry*, **13**(4) (2013).
39. I. Osasona, O. L. Faboya and A. O. Oso, *British J. Appl. Sci. Technol.*, **3**(4), 1006 (2013).
40. L. Zhou, J. Huang, B. He, F. Zhang and H. Li, *Carbohydr. Polym.*, **101**, 574 (2014).